# Radiotheranostics coupled between an At-211-Labeled RGD peptide and the corresponding radioiodine-labeled RGD peptide


| メタデータ | 言語: eng<br>出版者:<br>公開日: 2022-01-28<br>キーワード (Ja):<br>キーワード (En):<br>作成者:<br>メールアドレス:<br>所属: |
| --- | --- |
| URL | https://doi.org/10.24517/00065250 |

This work is licensed under a Creative Commons Attribution-NonCommercial-ShareAlike 3.0 International License.

This is an open access article published under an ACS AuthorChoice License, which permits copying and redistribution of the article or any adaptations for non-commercial purposes.

ACS OMEGA

Article

Cite This: ACS Omega 2019, 4, 4584−4591

http://pubs.acs.org/journal/acsodf

# Radiotheranostics Coupled between an At-211-Labeled RGD Peptide and the Corresponding Radioiodine-Labeled RGD Peptide

Kazuma Ogawa,*[,†,‡] Takuya Takeda,[‡] Kenji Mishiro,[†] Atsushi Toyoshima,[§] Kazuhiro Shiba,[∥] Takashi Yoshimura,[⊥] Atsushi Shinohara,[#] Seigo Kinuya,[‡] and Akira Odani[‡]

[†]Institute for Frontier Science Initiative and [‡]Graduate School of Medical Sciences, Kanazawa University, Kanazawa 920-1192, Japan

[§]Division of Science, Institute for Radiation Sciences, Osaka University, Toyonaka 560-0043, Japan

[∥]Advanced Science Research Center, Kanazawa University, Kanazawa 920-8640, Japan

[⊥]Radioisotope Research Center, Institute for Radiation Sciences, Osaka University, Suita 565-0871, Japan

[#]Graduate School of Science, Osaka University, Osaka 560-0043, Japan

*Supporting Information*

**ABSTRACT:** Alpha particle-emitting radionuclides have gained considerable attention for radionuclide therapy. Astatine-211 ($^{211}$At) is a promising alpha particle-emitting radionuclide. $^{211}$At is a halogen that has similar chemical properties to iodine and exhibits a half-life of 7.2 h. However, direct labeling of proteins or peptides into the tyrosine residue with $^{211}$At was shown to be impractical. Herein, we demonstrate a novel $^{211}$At-labeling method using the RGD peptide as a model peptide. An $^{211}$At-labeled RGD peptide, [$^{211}$At]c[RGDf(4-At)K], was prepared from a precursor with a tributylstannyl group on the phenylalanine residue in c(RGDfK) with a radiochemical yield of 63% and a radiochemical purity of >96%, and its potential for targeted radionuclide therapy was evaluated. Based on the results of biodistribution experiments, [$^{125}$I]c[RGDf(4-I)K] and [$^{211}$At]c[RGDf(4-At)K] showed high accumulation in the tumor and similar biodistribution. This study provides useful information for radiotheranostics between an $^{211}$At-labeled peptide and the corresponding radioiodine-labeled peptide.

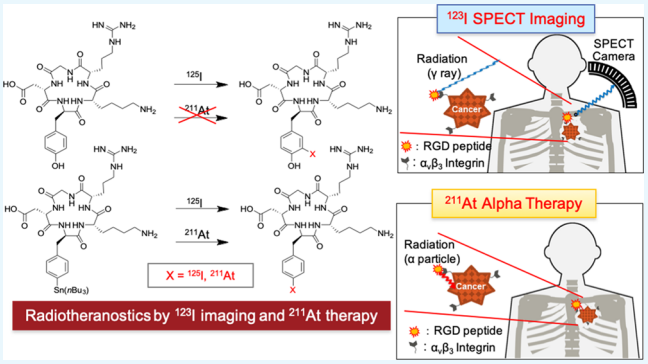


## INTRODUCTION

In recent years, the word "theranostics", a portmanteau of the words "therapeutics" and "diagnostics", has gathered much attention in oncological nuclear medicine. "Theranostics" implies the combination of both diagnosis and therapy. Effective use of radioisotope (RI)-labeled probes is one means of establishing a theranostics system, which is called as "radiotheranosticas".[1] RIs comprise not only radionuclides that emit radiation suitable for diagnosis (highly permeable gamma rays) but also radionuclides that emit radiation suitable for treatment ($\beta^-$-particles and $\alpha$-particles with high cytotoxicity). Some diagnostic and therapeutic RIs exhibit similar chemical properties. Therefore, diagnostic and therapeutic probes with equivalent pharmacokinetics can be prepared by introducing a diagnostic and therapeutic RI, respectively, that exhibit similar chemical properties, into the same precursor molecule. By coupling between the diagnostic and therapeutic probes, quantitative analyses by positron emission tomography (PET) or single-photon emission computed tomography (SPECT) after administration of the diagnostic probe should make it possible to estimate the absorbed radiation dose for therapeutic probes for each organ. Namely, imaging using the diagnostic probes can quantitatively predict the therapeutic effects and side effects of therapeutic probes. The radiotheranostics system is a likely method to realize personalized medicine because appropriate selection of patients and optimization of doses for therapy can give patients significant benefit, such as improved patient outcome and also yield health economic benefits.

Targeted radionuclide therapy that relies on administration of high energy radiation, such as alpha particles and beta particles, emitting RI-labeled probes is a therapeutic part in radiotheranostics. Examples of RIs include elements such as $^{131}$I and $^{89}$Sr, which have been used for decades, while RI-labeled carrier molecules have also been demonstrated for targeting of specific tissues. Examples of carriers used for targeted radionuclide therapeutics include antibodies, known as radioimmunotherapy,[2] peptides such as octreotide analogs,[3] and small molecules such as prostate-specific membrane antigen ligands[4] and benzylguanidine analogs [e.g., metaiodobenzylguanidine].[5]

Received: December 30, 2018
Accepted: February 12, 2019
Published: March 1, 2019

Downloaded via KANAZAWA UNIV on January 28, 2022 at 06:08:14 (UTC).
See https://pubs.acs.org/sharingguidelines for options on how to legitimately share published articles.

**Scheme 1. Preparation of [$^{125}$I]c[RGDf(4-I)K] (4) and [$^{211}$At]c[RGDf(4-At)K] (5) via the Tributyltin Precursor, c{RGDf[4-Sn(*n*Bu)$_3$]K} (3). Reagents: (a) TFA, Triisopropylsilane, $H_2O$, (b) [(*n*Bu)$_3$Sn]$_2$, Tris(dibenzylideneacetone)dipalladium(0), *N*,*N*-Diisopropylethylamine (DIEA) (c) [$^{125}$I]NaI, *N*-Chlorosuccinimide, or [$^{211}$At]At$^-$, *N*-Chlorosuccinimide**

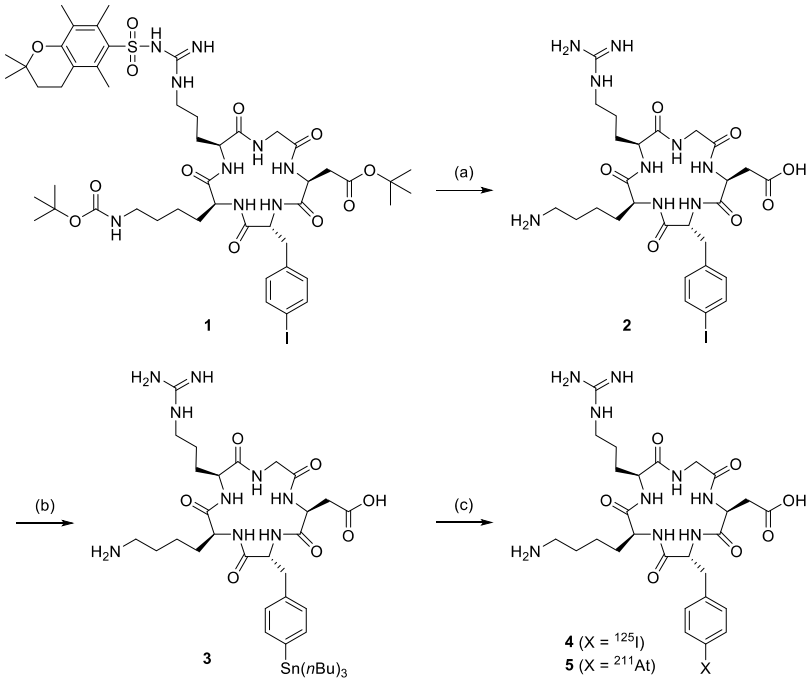


Alpha particle-emitting radionuclides have gained considerable attention for use in radionuclide therapy because of the high linear energy transfer of the alpha particle. For example, Ra-223 showed excellent therapeutic effects in a phase III study for castration-resistant prostate cancer patients with bone metastases[6] and has been approved in the US, EU, and many other countries. Other alpha-emitting RIs, such as $^{211}$At, $^{213}$Bi, $^{225}$Ac, and $^{227}$Th, have been enthusiastically investigated, with some studies offering promise toward clinical use in the future.[7,8] Among the alpha-emitting radionuclides, astatine-211 ($^{211}$At) has gained considerable attention. $^{211}$At decays, with a half-life that is appropriate for alpha therapy ($t_{1/2}$ = 7.2 h), to $^{207}$Bi (42%) with emission of $\alpha$-particles (5.9 MeV) or $^{211}$Po (58%) via electron capture. Subsequently, $^{207}$Bi ($t_{1/2}$ = 33.9 years) decays to $^{207}$Pb via electron capture and $^{211}$Po ($t_{1/2}$ = 516 ms) decays to $^{207}$Pb with an emission of $\alpha$-particles (7.5 MeV). Moreover, astatine, the 85th element in the periodic table, is a halogen, and exhibits similar chemical properties to those of iodine.

$^{211}$At-based targeted alpha therapy has mainly been investigated using antibodies as carriers to the targeted cancer.[9−11] It is known that peptides, such as the above-mentioned octreotide analogs for neuroendocrine tumors,[12] cyclic pentapeptides containing an RGD (Arg-Gly-Asp) motif known as a typical ligand for $\alpha_v\beta_3$ integrin,[13] which is a heterodimeric transmembrane receptor for cell adhesion and was identified as a marker of angiogenic blood vessels,[14] bombesin analogs as ligands for gastrin-releasing peptide receptor overexpressed in various types of cancer (e.g., prostate cancer and breast cancer),[15] and so on, have also been reported as useful carriers for radiotheranostics. However, there are only a few reports on $^{211}$At-labeled octreotide analogs and substance P (5−11),[16−18] while investigations of $^{211}$At-labeled peptides containing an RGD motif have not been reported.

For radioiodine labeling of peptides containing tyrosine residues, such as c(RGDyK) or antibodies, the simplest and most effective method of introducing a radioiodine at the 3-position on the tyrosine residue is the chloramine-T method, which typically results in high radiochemical yields.[19,20] Moreover, owing to the small size of the iodine molecule, introduction of iodine has little effect on the bioactivity and biodistribution compared to other labeling reagents, such as fluorescent groups, or indirect radioiodine labeling.[21] In contrast to iodine, direct labeling of antibodies into the tyrosine residue with $^{211}$At was shown to be impractical,[22] and $^{211}$At might not be introduced into the tyrosine residue of c(RGDyK) via the normal chloramine-T method.

In this study, we used an RGD-containing peptide as a model for establishing a novel $^{211}$At-labeling method for peptides. The $^{211}$At-labeled RGD peptide, [$^{211}$At]c[RGDf(4-At)K] (**5**), was prepared from a precursor (**3**) containing a tributylstannyl group on the phenylalanine residue in c-(RGDfK) (Scheme 1) because $^{211}$At labeling can be performed by a standard halogenation reaction using the corresponding tributylstannyl precursor.[23] The applicability of the novel $^{211}$At-labeling method and the $^{211}$At-labeled RGD peptide were evaluated by in vitro and in vivo experiments and compared with the corresponding $^{125}$I-labeled RGD peptide, [$^{125}$I]c-[RGDf(4-I)K] (**4**) for establishing radiotheranostics by coupling between $^{123}$I for SPECT imaging and $^{211}$At for $\alpha$ therapy. Although we are interested in $^{123}$I ($t_{1/2}$ = 12.3 h) for SPECT imaging, $^{125}$I ($t_{1/2}$ = 59.4 d) was used in this basic study as an alternative radionuclide because of its long half-life.

## ■ RESULTS

**Preparation of an $^{211}$At-Labeled Peptide [$^{211}$At]c-[RGDf(4-At)K] (5).** We first synthesized Fmoc-D-4-iodophenylalanine, followed by synthesis of cyclic[Arg(Pbf)-Gly-Asp(O*t*Bu)-D-Phe(4-I)-Lys(Boc)] (**1**) by Fmoc solid-phase



DOI: 10.1021/acsomega.8b03679
ACS Omega 2019, 4, 4584−4591

synthesis. We then replaced the iodine molecule by a tributylstannyl group via the stannylation reaction (Scheme S1), as we had anticipated the stannylation reaction to be difficult to carry out after deprotection of the amino acid-protecting groups. Using this methodology, we planned to prepare [$^{211}$At]c[RGDf(4-At)K] by deprotection of the protecting groups following $^{211}$At-labeling via the astatodestannylation reaction. $^{211}$At-labeling was performed at a high radiochemical yield (87%). Deprotection following $^{211}$At-labeling initially failed when using the same method as that used for preparation of [$^{125}$I]c[RGDf(4-I)K]. Shorting the reaction time of deprotection with trifluoroacetic acid (TFA) made the preparation of [$^{211}$At]c[RGDf(4-At)K] possible. However, the yield of the deprotection step was low (38%) and the 2-step reaction was suggested to be unfavorable, given the complications and the operation time required for clinical use. We therefore sought to prepare [$^{211}$At]c[RGDf(4-At)K] by a 1-step reaction from the tributylstannyl precursor without protecting groups. Specifically, the tributylstannyl group was successfully introduced to the nonprotected peptide under the Pd-catalyzed stannylation condition reported by Pickett et al.[24] with a slight modification (Scheme 1). $^{211}$At-labeling was then performed via the astatodestannylation reaction in a simple 1-step reaction with a moderate radiochemical yield (63%).

**Determination of the Partition Coefficient and HPLC Analyses.** As astatine has no stable isotopes, the lack of a reference nonradioactive At-labeled peptide limited our ability to determine the chemical structure of the resultant $^{211}$At-labeled peptide. In this study, the identity of [$^{211}$At]c[RGDf(4-At)K] was verified by comparing its retention time with that of nonradioactive c[RGDf(4-I)K] (Figure S1). Similar retention times for [$^{211}$At]c[RGDf(4-At)K] and c[RGDf(4-I)K] in the corresponding HPLC chromatograms were consistent with similar log *P* values from the partition coefficient experiments of [$^{125}$I]c[RGDf(4-I)K] and [$^{211}$At]c[RGDf(4-At)K] (−3.04 ± 0.46 and −3.00 ± 0.02, respectively), suggesting that the estimated chemical structure of [$^{211}$At]c[RGDf(4-At)K] (Scheme 1, **5**) was aligned with these results.

**$\alpha_v\beta_3$ Integrin Binding Assay.** The affinity of c[RGDf(4-I)K] and c(RGDfK) for the $\alpha_v\beta_3$ integrin was determined in a competitive binding assay. Representative results of the assay are shown in Figure 1. Binding of [$^{125}$I]c[RGDy(3-I)K] to $\alpha_v\beta_3$ was competed by c[RGDf(4-I)K] and c(RGDfK) in a concentration-dependent manner. The half maximal inhibitory concentration ($IC_{50}$) values (nM) of c[RGDf(4-I)K] and c(RGDfK) were 30.8 ± 7.9 and 14.6 ± 8.7, respectively. These values were not statistically significant. Thus, introduction of an iodine molecule into the phenylalanine residue did not significantly impede the affinity of c(RGDfK) for the $\alpha_v\beta_3$ integrin.

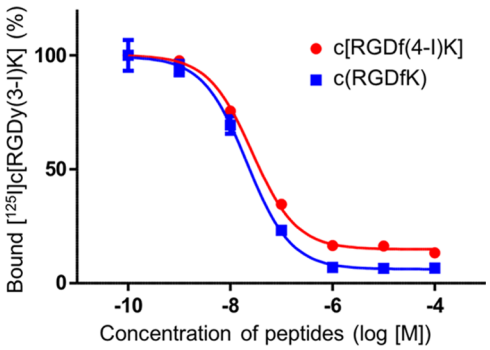


**Figure 1.** Integrin binding assay. Representative displacement curves of the competitive binding to the $\alpha_v\beta_3$ integrin of [$^{125}$I]c[RGDy(3-I)K] with c(RGDfK) and c[RGDf(4-I)K]. Error bars represent standard deviation (SD).

Competitive binding experiments of [$^{211}$At]c[RGDf(4-At)K] to the $\alpha_v\beta_3$ integrin were also performed because there are no stable isotopes of astatine. Binding of [$^{211}$At]c-[RGDf(4-At)K] to the $\alpha_v\beta_3$ integrin decreased in c(RGDfK) peptide concentration-dependent manner (Figure S3).

**Animal Experiments.** In this study, [$^{125}$I]c[RGDf(4-I)K] and [$^{211}$At]c[RGDf(4-At)K] were co-injected into tumor-bearing mice to minimize the number of mice and experimental errors. Results of the biodistribution experiments of [$^{125}$I]c[RGDf(4-I)K] and [$^{211}$At]c[RGDf(4-At)K] in U-87 MG tumor-bearing mice are shown in Table 1. The biodistribution of [$^{125}$I]c[RGDf(4-I)K] and [$^{211}$At]c[RGDf-(4-At)K] showed very similar patterns, such as high tumor uptake and low uptake in stomach and other nontarget tissues, except the kidney and the intestine for excretion.

**Table 1. Biodistribution of Radioactivity after Concomitant Intravenous Injection of [$^{125}$I]c[RGDf(4-I)K] and [$^{211}$At]c[RGDf(4-At)K] in U-87 MG Tumor-Bearing Mice**[a,c]

| tissue | time after injection | | |
|---|---|---|---|
| | 1 h | 4 h | blocking (1 h) |
| | [$^{125}$I]c[RGDf(4-I)K] | | |
| blood | 0.65 (0.07) | 0.19 (0.03) | 0.73 (0.11) |
| liver | 3.06 (0.48) | 1.79 (0.56) | 2.47 (0.33) |
| kidney | 9.15 (1.49) | 4.89 (0.97) | 6.62 (1.79) |
| small intestine | 5.59 (0.60) | 3.22 (1.21) | 2.15 (0.17)** |
| large intestine | 1.70 (0.37) | 6.73 (4.58) | 0.25 (0.05)** |
| spleen | 1.40 (0.28) | 1.19 (0.13) | 0.30 (0.04)** |
| pancreas | 0.92 (0.15) | 0.70 (0.14) | 0.35 (0.04)** |
| lung | 1.40 (0.27) | 0.72 (0.18) | 0.67 (0.14)** |
| heart | 0.80 (0.13) | 0.39 (0.04) | 0.34 (0.03)** |
| stomach[b] | 0.50 (0.18) | 0.24 (0.02) | 0.18 (0.06)* |
| bone | 0.81 (0.15) | 0.58 (0.09) | 0.31 (0.04)** |
| muscle | 0.52 (0.20) | 0.27 (0.06) | 0.20 (0.04)* |
| brain | 0.12 (0.04) | 0.08 (0.02) | 0.05 (0.00)* |
| tumor | 4.61 (1.26) | 2.93 (0.08) | 0.69 (0.08)** |
| | [$^{211}$At]c[RGDf(4-At)K] | | |
| blood | 0.65 (0.05) | 0.39 (0.10) | 0.77 (0.12) |
| liver | 2.82 (0.49) | 1.57 (0.54) | 2.56 (0.10) |
| kidney | 8.17 (0.46) | 4.65 (0.64) | 6.73 (0.73)* |
| small intestine | 5.77 (0.56) | 2.44 (0.24) | 2.83 (0.20)** |
| large intestine | 1.96 (0.41) | 6.08 (1.90) | 0.36 (0.12)** |
| spleen | 2.00 (0.37) | 1.93 (0.26) | 0.83 (0.20)** |
| pancreas | 1.05 (0.23) | 0.95 (0.13) | 0.52 (0.02)* |
| lung | 2.00 (0.45) | 1.53 (0.39) | 1.20 (0.26)* |
| heart | 1.06 (0.21) | 0.70 (0.09) | 0.53 (0.06)** |
| stomach[b] | 0.63 (0.23) | 0.39 (0.01) | 0.29 (0.14) |
| bone | 0.97 (0.17) | 0.82 (0.16) | 0.46 (0.04)** |
| muscle | 0.58 (0.20) | 0.36 (0.08) | 0.24 (0.07)* |
| brain | 0.15 (0.04) | 0.11 (0.03) | 0.08 (0.01)* |
| tumor | 5.26 (1.46) | 3.21 (0.12) | 0.95 (0.15)** |

[a]Expressed as % injected dose per gram. Each value represents the mean (SD) for three or four animals. [b]Expressed as % injected dose. [c]Significance was determined by unpaired Student's *t*-test. *$P < 0.05$ vs control (1 h). **$P < 0.01$ vs control (1 h).



DOI: 10.1021/acsomega.8b03679
ACS Omega 2019, 4, 4584−4591

We evaluated whether accumulation of [$^{125}$I]c[RGDf(4-I)K] and [$^{211}$At]c[RGDf(4-At)K] in the tumor was $\alpha_v\beta_3$ integrin-specific. Figure 2 shows the tumor accumulation of [$^{125}$I]c-[RGDf(4-I)K] and [$^{211}$At]c[RGDf(4-At)K] at 1 h after injection with an excess of the RGD peptide. The results show that accumulation of [$^{125}$I]c[RGDf(4-I)K] and [$^{211}$At]-c[RGDf(4-At)K] in the tumor was significantly decreased upon co-injection with an excess of c(RGDfK), suggesting that the tumor accumulation of [$^{125}$I]c[RGDf(4-I)K]and [$^{211}$At]c-[RGDf(4-At)K] is caused by specific binding affinity for the $\alpha_v\beta_3$ integrin.

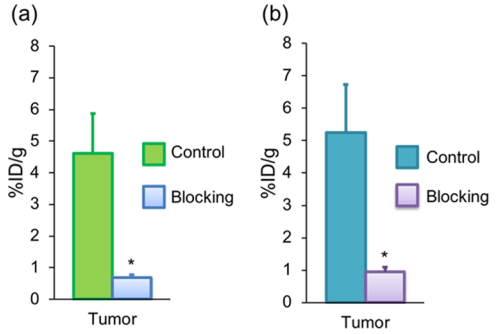


**Figure 2.** Blocking study. Comparison of tumor uptake (mean ± SD) of (a) [$^{125}$I]c[RGDf(4-I)K] and (b) [$^{211}$At]c[RGDf(4-At)K] at 1 h postinjection under no-carrier-added conditions and with co-injection of an excess of c(RGDfK). Significance was determined by unpaired Student's *t*-test (*$p < 0.05$, vs control).

## ■ DISCUSSION

Some methodologies have been reported for $^{211}$At-labeling of antibodies. For example, *closo*-decaborate(2−) derivatives were used as labeling agents and conjugated to the antibody prior to $^{211}$At-labeling.[25] The astatodestannylation reaction has also been used for antibody labeling both before and after conjugation. *N*-Succinimidyl 3-(tri-*n*-butylstannyl)benzoate (ATE) is one reagent commonly used for indirect labeling with halogens and has been used for radiolabeling of antibodies.[26,27] Specifically, both *N*-succinmidyl [$^{211}$At]-astatobenzoate ([$^{211}$At]SAB)-conjugated antibodies and ATE-conjugated antibodies followed by $^{211}$At-labeling via the astatodestannylation reaction have been demonstrated.[28,29] These methods, namely, $^{211}$At-labeling via conjugation of [$^{211}$At]SAB or ATE with the $\varepsilon$-amino group of lysine residues or the N-terminus of amino acid sequences, are applicable to both proteins and peptides. Therefore, we recently sought to synthesize $^{125}$I- and $^{77}$Br-labeled RGD peptides in which *N*-succinmidyl [$^{125}$I]iodobenzoate ([$^{125}$I]SIB) or *N*-succinmidyl [$^{77}$Br]bromobenzoate ([$^{77}$Br]SBrB) had been introduced via conjugation with the $\varepsilon$-amino group of the lysine residue in the c(RGDfK) peptide as a preliminary investigation into $^{211}$At-labeling of an RGD peptide.[20] Radiolabeling with both $^{125}$I and $^{77}$Br was successful; however, the biodistribution of the resultant-labeled RGD peptides was not favorable for use as radiopharmaceuticals, owing to extremely high uptake in the intestine and low tumor uptake, which can be due to the increased lipophilicity of these peptides. As the molecular sizes of peptides are much smaller compared to antibodies, the biodistribution of labeled peptides must be drastically affected by introduction of molecules containing benzene rings. Next, we prepared labeled RGD peptides containing a hydrophilic linker between the c(RGDfK) peptide and a radiolabeled site to decrease the lipophilicity of the resultant-labeled peptide. However, this method did not sufficiently improve the biodistribution. We therefore investigated another strategy for preparing $^{211}$At-labeled RGD peptide, namely, introduction of a tributylstannyl group (for subsequent halogen labeling) into the phenylalanine residue of the RGD peptide in this study.

Regarding $^{211}$At-labeling of the RGD peptide via the astatodestannylation reaction in this study, although the radiochemical yield using the simple 1-step reaction (Scheme 1, 63%) was much higher than that resulting from the 2-step reaction (Scheme S1, 33%), it was lower than that previously reported astatodestannylation reaction (91%)[23] as well as that of the abovementioned first labeling reaction (87%) via a 2-step reaction. Although the reason is not clear, these results suggested that the functional groups of the amino acid residues in c(RGDfK) might impede efficient radiolabeling.

It has been known that some RIs are useful for radiotheranostics. Some radiometals, which can form stable complexes with the same ligand, such as $^{99m}$Tc for diagnosis and $^{186/188}$Re for therapy using the mercaptotriglysine (MAG3) ligand or tricarbonyl ligand,[30,31] or $^{111}$In and $^{67/68}$Ga for diagnosis and $^{90}$Y, $^{177}$Lu, $^{213}$Bi, and $^{225}$Ac for therapy using the 1,4,7,10-tetraazacyclododecane-1,4,7,10-tetraacetic acid ligand could be useful as a theranostics system.[32] In this concept, forming stable complexes is very important for similar biodistribution between a diagnostic probe and a therapeutic probe for use of radiotheranostics. Meanwhile, as iodine and astatine are halogen elements and iodine- and astatine-labeled probes would likely show similar biodistribution, the coupling between $^{123}$I for SPECT imaging and $^{211}$At for $\alpha$ therapy could also be applicable as a theranostics system. In this case also, to guarantee the stability of both radiolabeled probes for imaging and therapy is very important to succeed the radiotheranostics. However, some astatine-labeled probes are easier to decompose than iodine-labeled probes because of their lower stability,[33] for example, it was reported that more dehalogenation (deastatination) from astatine-labeled Fab via [$^{211}$At]SAB or its catabolite occurred compared with that (deiodination) from iodine-labeled one via [$^{125}$I]SIB.[28] Meanwhile, in this study, $^{211}$At- and $^{125}$I-labeled RGD peptides showed very similar biodistribution based on their high stability in vivo and high affinity for the $\alpha_v\beta_3$ integrin. It is the most important outcome in this study. The low uptake of [$^{125}$I]c[RGDf(4-I)K] and [$^{211}$At]c[RGDf(4-At)K] in the stomach indicates that in vivo dehalogenation of [$^{125}$I]c-[RGDf(4-I)K] and [$^{211}$At]c[RGDf(4-At)K] did not occur because iodide and astatide ions are known to highly accumulate in the stomach.[34,35] These results indicated that SPECT imaging using [$^{123}$I]c[RGDf(4-I)K] could allow for prediction of the therapeutic effects and side effects of [$^{211}$At]c[RGDf(4-At)K] as the radiotheranostics system.

Co-injection of radiotracers with excess amount of the c(RGDfK) peptide (0.2 mg/mouse) drastically decreased tumor uptake of the tracer. It also significantly reduced the accumulation of radioactivity in many kinds of normal tissues (Table 1). Similar results with regard to other radiolabeled RGD peptides were reported.[13,36] It has been reported that the $\alpha_v\beta_3$ integrin is expressed in not only angiogenic blood vessels and tumor cells but also microvessels in normal tissues, such as lung, and normal cells, such as osteoclast.[37,38] Therefore, the results of the blocking study suggest some parts of


DOI: 10.1021/acsomega.8b03679
ACS Omega 2019, 4, 4584−4591

accumulation in the normal tissues should be via the $\alpha_v\beta_3$ integrin. These results do not seem to contradict with previous reports.

## CONCLUSIONS

The $^{211}$At-labeled RGD peptide prepared in this study showed high stability and similar biodistribution in vivo to the corresponding $^{125}$I-labeled RGD peptide. Therefore, this study provides useful information for the $^{211}$At-labeling method of peptides and for the application of coupling between $^{123}$I- and $^{211}$At-labeled peptides for radiotheranostics. This method could be applicable to other peptides directly targeted to cancer. Moreover, future efforts should be focused on application of other radiohalogens, such as $^{18}$F and $^{76}$Br as positron emitters for PET imaging as well as preparation and evaluation of other $^{211}$At-labeled peptides, to confirm the application of the concept for "radiotheranostics".

## MATERIALS AND METHODS

**Materials.** [$^{125}$I]Sodium iodide (644 GBq/mg) was purchased from PerkinElmer (Waltham, MA, USA). Electrospray ionization mass spectra (ESI−MS) were obtained with a JEOL JMS-T100TD (JEOL Ltd., Tokyo, Japan). Purification of peptides was performed using an HPLC system (LC-20AD pump, SPD-20A UV detector at a wavelength of 220 nm, and CTO-20A column oven maintained at 40 °C; Shimadzu, Kyoto, Japan). Thin layer chromatography analyses were performed with silica plates (Art 5553, Merck, Darmstadt, Germany). Fmoc-Lys(Boc)-OH was purchased from Merck (Darmstadt, Germany). 2-Chlorotrityl chloride resin, Fmoc-Arg(Pbf)-OH, Fmoc-Asp(O*t*Bu)-OH, Fmoc-Gly-OH, Fmoc-D-Tyr(*t*Bu)-OH, and Fmoc-D-Phe-OH were purchased from Watanabe Chemical Industries, Ltd. (Hiroshima, Japan). Fmoc-4-iodo-D-phenylalanine [Fmoc-D-Phe(4-I)] was synthesized according to a previous report.[39] DIEA was purchased from Nacalai Tesque (Kyoto, Japan). 1,3-Diisopropylcarbodiimide and 1-hydroxybenzotriazole hydrate were purchased from Kokusan Chemical Co., Ltd. (Tokyo, Japan). Other reagents were of reagent grade and used as received.

**Production of Astatine-211.** Astatine-211 was produced via the $^{209}$Bi($\alpha$, 2$n$)$^{211}$At reaction using the AVF cyclotron at the Research Center for Nuclear Physics (RCNP), Osaka University. A 20 mg/cm$^2$ metallic Bi target prepared by vacuum evaporation was placed at 45° to the beam axis and was irradiated with a 27.3 MeV $\alpha$ beam. Typical $^4$He$^{2+}$ beam current was 1.0 particle $\mu$A. During irradiation, the Bi target was cooled with circulating water and helium gas.

$^{211}$At was isolated from the irradiated target materials by dry distillation. The distillation was carried out in a quartz tube at 850 °C in helium/oxygen mixed gas. Distilled $^{211}$At was deposited in a cooled Teflon tube connected to the quartz tube and was then recovered with approximately 100 $\mu$L of distilled water in a small plastic vial by washing the inside of the Teflon tube. Gamma-ray spectrometry of the $^{211}$At sample was performed using a Ge detector before and after the distillation to determine the radioactivity.

Approximately, 30 MBq of $^{211}$At was produced by each irradiation. After dry-distillation, 10−20 MBq of $^{211}$At was obtained at a chemical yield of 70−80%. $^{210}$At was not detected in either of the irradiated targets. In $^{211}$At solution, no radioactivity except for $^{211}$At was detected and the contamination factors were evaluated to be $^{210}$At/$^{211}$At < $10^{-4}$ and $^{210}$Po/$^{211}$At < $10^{-6}$; $^{210}$At and $^{210}$Po are most possible nuclides contained in the solution sample. Thus, the radionuclide purity of $^{211}$At is >99.99%. Possible stable nuclides (elements) which could be included in the solution are Bi and Al. We have not determined contamination factors of these elements, but basically, these nonvolatile elements can be completely separated in the dry distillation process adapted in the present study.

**Preparation of c[RGDf(4-I)K] (2).** Peptide synthesis was performed manually using a standard Fmoc-based solid-phase methodology according to a previous report (Scheme 1).[20,40]

c[R(Pbf)GD(O*t*Bu)f(4-I)K(Boc)] (**1**) was purified by reversed-phase (RP)-HPLC performed with a Cosmosil 5C$_{18}$-AR-II column (10 × 150 mm; Nacalai Tesque, Kyoto, Japan) at a flow rate of 4.0 mL/min with a gradient mobile phase of 80% methanol in water with 0.1% TFA to 90% methanol in water with 0.1% TFA for 20 min. The fraction containing c[R(Pbf)GD(O*t*Bu)f(4-I)K(Boc)] (**1**) was determined by mass spectrometry and collected. The solvent was removed by lyophilization to yield c[R(Pbf)GD(O*t*Bu)f(4-I)K(Boc)] (**1**) (64 mg, 37%) as white powder. c[R(Pbf)GD(O*t*Bu)f(4-I)K(Boc)] (**1**): HRMS (ESI+) calcd for $C_{49}H_{73}IN_9O_{12}S$ [M + H]$^+$: $m/z$, 1138.4144; found, 1138.4138.

c[R(Pbf)GD(O*t*Bu)f(4-I)K(Boc)] (**1**) (10 mg, 8.8 $\mu$mol) was treated with 95% TFA, 2.5% water, and 2.5% triisopropylsilane for 2 h at room temperature. The crude peptide was purified by reversed-phase high-performance liquid chromatography (RP-HPLC) performed with a Cosmosil 5C$_{18}$-AR-II column (10 × 150 mm) at a flow rate of 4.0 mL/min with a gradient mobile phase of 30% methanol in water with 0.1% TFA to 50% methanol in water with 0.1% TFA for 20 min. The fraction containing c[RGDf(4-I)K] (**2**) was determined by mass spectrometry and collected. The solvent was removed by lyophilization to yield c[RGDf(4-I)K] (**2**) (6.1 mg, 95%) as white powder. c[RGDf(4-I)K] (**2**): HRMS (ESI+) calcd for $C_{27}H_{41}IN_9O_7$ [M + H]$^+$: $m/z$, 730.2174; found, 730.2158.

**Preparation of c{RGDf[4-Sn(*n*Bu)$_3$]K} (3).** Compound **2** (2.0 mg, 2.7 $\mu$mol) was dissolved in 400 $\mu$L of methanol. Bis(tributyltin) (5.8 $\mu$L, 11.8 $\mu$mol), tris(dibenzylideneacetone)dipalladium(0) (384 $\mu$g, 419 nmol), and DIEA (1.2 $\mu$L, 6.9 $\mu$mol) were added to the solution of compound **2** under a $N_2$ atmosphere. After 12 h stirring at 60 °C, the reaction mixture was purified by RP-HPLC with a Cosmosil 5C$_{18}$-AR-II column (10 × 150 mm) at a flow rate of 4.0 mL/min with a gradient mobile phase of 70% methanol in water with 0.1% TFA to methanol in water with 0.1% TFA for 10 min. The fraction containing c{RGDf[4-Sn($n$Bu)$_3$]K} (**3**) was determined by mass spectrometry and collected. The solvent was removed by lyophilization to yield c{RGDf[4-Sn($n$Bu)$_3$]K} (**3**) (612 $\mu$g, 25%) as white powder. c{RGDf[4-Sn($n$Bu)$_3$]K} (**3**): HRMS (ESI+) calcd for $C_{39}H_{68}N_9O_7Sn$ [M + H]$^+$: $m/z$, 894.4264; found, 894.4258.

**Preparation of [$^{125}$I]c[RGDf(4-I)K] (4).** Compound **3** (30 $\mu$g, 33.6 nmol) was dissolved in 5 $\mu$L of acetonitrile in the reaction vial. 10 $\mu$L of 1% acetic acid in acetonitrile, 3 $\mu$L of [$^{125}$I]NaI (3.7 MBq) solution, and 15 $\mu$L of *N*-chlorosuccinimide (NCS) in acetonitrile (1 mg/mL) were added to the vial. After heating for 15 min at 80 °C, the reaction mixture was quenched with 15 $\mu$L of $NaHSO_3$ solution (1 mg/mL) and then purified by RP-HPLC with a Cosmosil 5C$_{18}$-AR-II column (4.6 × 150 mm) at a flow rate of 1 mL/min with an isocratic mobile phase of 30% methanol in water with 0.1%


DOI: 10.1021/acsomega.8b03679
ACS Omega 2019, 4, 4584−4591

TFA. The retention time of **4** was 9 min (Figure S1). The specific activity of **4** was theoretically calculated as 111 MBq/mg because the separation between **4** and precursor **3**, which was not eluted until 20 min in this HPLC condition, was complete. The radiochemical yields of **4** was 83%. The radiochemical purity of **4** was >95%.

**Preparation of [$^{211}$At]c[RGDf(4-At)K] (5).** Compound **3** (30 $\mu$g, 33.6 nmol) was dissolved in 5 $\mu$L of acetonitrile in the reaction vial. 10 $\mu$L of 1% acetic acid in acetonitrile, 100 $\mu$L of [$^{211}$At]At$^-$ aqueous solution (7.4 MBq), and 15 $\mu$L of NCS in acetonitrile (1 mg/mL) were added to the vial. After heating for 15 min at 80 °C, the reaction mixture was quenched with 15 $\mu$L of $NaHSO_3$ solution (1 mg/mL) and then purified by RP-HPLC with a Cosmosil 5$C_{18}$-AR-II column (4.6 × 150 mm) at a flow rate of 1 mL/min with an isocratic mobile phase of 30% methanol in water with 0.1% TFA. The retention time of **5** was 10 min (Figure S1). The specific activity of **5** was theoretically calculated as 19.8 TBq/mg because the separation between **5** and precursor **3** was complete. The radiochemical yields of **5** was 63%. The radiochemical purity of **5** was >95%.

**Preparation of [$^{125}$I]c[RGDf(4-I)K] (4) and [$^{211}$At]c-[RGDf(4-At)K] (5) by Two-Step Labeling.** Two-step labeling methods for [$^{125}$I]c[RGDf(4-I)K] (**4**) and [$^{211}$At]c-[RGDf(4-At)K] (**5**) were performed according to Scheme S1. c[R(Pbf)GD(O*t*Bu)f(4-I)K(Boc)] (**1**) (5.6 mg, 4.9 $\mu$mol) was dissolved in 400 $\mu$L of anhydrous 1,4-dioxane. Bis(tributyltin) (6.0 $\mu$L, 11.8 $\mu$mol) and bis(triphenylphosphine)palladium(II) dichloride (0.52 $\mu$L, 0.74 $\mu$mol) were added to the compound **1** solution under a $N_2$ atmosphere. After 2 h stirring at 60 °C, the reaction mixture was purified by RP-HPLC performed with a Cosmosil 5$C_{18}$-AR-II column (10 × 150 mm) at a flow rate of 4.0 mL/min with a gradient mobile phase of 95% methanol in water with 0.1% TFA to 100% methanol with 0.1% TFA for 20 min. The fraction containing compound **6** was determined by mass spectrometry and collected. The solvent was removed by lyophilization to provide c{R(Pbf)GD(O*t*Bu)f[4-Sn-(*n*Bu)$_3$]K(Boc)} (**6**) (512 $\mu$g, 8%) as white powder.

HRMS (ESI+) calcd for $C_{61}H_{99}N_9NaO_{12}SSn$ [M + Na]$^+$: *m*/*z*, 1324.6054; found, 1324.6034.

Compound **6** (30 $\mu$g, 23.0 nmol) was dissolved in ethanol (79 $\mu$L). Chloramine-T in ethanol (1 mg/mL, 15 $\mu$L), 1% acetic acid in ethanol (21 $\mu$L), and [$^{125}$I]NaI (3.7 MBq, 3 $\mu$L) were added to compound **6** solution. After 15 min standing at room temperature, compound **7** was obtained after RP-HPLC purification with a Cosmosil 5$C_{18}$-AR-II column (4.6 × 150 mm) at a flow rate of 1 mL/min with a gradient mobile phase of 80% methanol in water with 0.1% TFA to 100% methanol with 0.1% TFA. The radiochemical yield was 83%. The radiochemical purity was over 95%.

Compound **7** was treated with 95% TFA, 2.5% water, and 2.5% triisopropylsilane for 90 min at room temperature. After removal of solvents using $N_2$ gas, the residue was purified by RP-HPLC with a Cosmosil 5$C_{18}$-AR-II column (4.6 × 150 mm) at a flow rate of 1.0 mL/min with a gradient mobile phase of 30% methanol in water with 0.1% TFA to 70% methanol in water with 0.1% TFA for 20 min. The radiochemical yield was 75%. The radiochemical purity was over 95%.

Compound **6** (30 $\mu$g, 23.0 nmol) was dissolved in 5 $\mu$L of acetonitrile in the reaction vial. 10 $\mu$L of 1% acetic acid in acetonitrile, 3 $\mu$L of [$^{211}$At]At$^-$ aqueous solution (3.7 MBq), and 15 $\mu$L of NCS in acetonitrile (1 mg/mL) were added to the vial. After 15 min heating at 80 °C, the reaction mixture was quenched with 15 $\mu$L of $NaHSO_3$ solution (1 mg/mL).

Compound **8** was treated with 95% TFA, 2.5% water, and 2.5% triisopropylsilane for 10 min at room temperature. After removal of solvents using $N_2$ gas, the residue was purified by RP-HPLC with a Cosmosil 5$C_{18}$-AR-II column (4.6 × 150 mm) at a flow rate of 1.0 mL/min with an isocratic mobile phase of 30% methanol in water with 0.1% TFA. The radiochemical yield was 37%. The radiochemical purity was over 95%.

**Determination of the Partition Coefficient.** The partition coefficients of [$^{125}$I]c[RGDf(4-I)K] and [$^{211}$At]c-[RGDf(4-At)K] were measured as described previously.[41] The partition coefficient was determined by calculating the ratio of cpm/mL in 1-octanol to that in buffer and expressed as a common logarithm (log *P*).

**$\alpha_v\beta_3$ Integrin Binding Assay.** Binding affinities of synthesized peptides, c[RGDf(4-I)K] and c(RGDfK), for the $\alpha_v\beta_3$ integrin were evaluated by competitive inhibition between the peptides and [$^{125}$I]c[RGDy(3-I)K] to the $\alpha_v\beta_3$ integrin according to a previously reported procedure.[20,40]

**Biodistribution Experiments of [$^{125}$I]c[RGDf(4-I)K] and [$^{211}$At]c[RGDf(4-At)K] in Tumor-Bearing Mice.** Experiments with animals were conducted in strict accordance with the Guidelines for the Care and Use of Laboratory Animals of Kanazawa University. The experimental protocols were approved by the Committee on Animal Experimentation of Kanazawa University. The animals were housed with free access to food and water at 23 °C with a 12 h alternating light/dark schedule. The U-87 MG glioblastoma cell line was obtained from DS Pharma Biomedical (Osaka, Japan). U-87 MG cells were grown and injected subcutaneously into 4-week-old female BALB/c nude mice (15−19 g, Japan SLC, Inc., Hamamatsu, Japan) as previously reported.[40] Biodistribution experiments were performed approximately 14−21 days postinoculation, that is, the time needed for tumors to reach a palpable size. A mixed solution of [$^{125}$I]c[RGDf(4-I)K] (37 kBq) and [$^{211}$At]c[RGDf(4-At)K] (37 kBq) was intravenously administered to groups of three or four mice. Mice were sacrificed at 1 and 4 h postinjection. Tissues of interest were removed and weighed, and radioactivity counts of $^{125}$I and $^{211}$At were determined with an auto-well gamma counter (Wallac Wizard 1470 Gamma Counter, PerkinElmer) and corrected for background radiation. A window from 1 to 80 keV was used for counting $^{125}$I and a window from 70 to 120 keV was used for counting $^{211}$At. Correlation factors to eliminate any crossover of $^{125}$I activity in the $^{211}$At counts were determined by measuring the $^{125}$I standard in both windows. More than one week after the experiments, the radioactivity counts of $^{125}$I were measured after attenuation of $^{211}$At.

To investigate the effect of an excess amount of the RGD peptide on biodistribution as a blocking study, 100 $\mu$L of a mixed solution of [$^{125}$I]c[RGDf(4-I)K] (37 kBq), [$^{211}$At]c-[RGDf(4-At)K] (37 kBq) and c(RGDfK) peptide (0.2 mg/mouse) was intravenously injected into U87MG tumor-bearing mice. Mice ($n$ = 4) were sacrificed at 1 h postinjection, and biodistribution experiments were conducted as described above.



DOI: 10.1021/acsomega.8b03679
ACS Omega 2019, 4, 4584−4591

## ■ ASSOCIATED CONTENT

### Supporting Information

The Supporting Information is available free of charge on the ACS Publications website at DOI: 10.1021/acsomega.8b03679.

Synthesis scheme of [$^{125}$I]c[RGDf(4-I)K] (**4**) and [$^{211}$At]c[RGDf(4-At)K] (**5**) by a two-step labeling method (Scheme S1), RP-HPLC chromatograms (Figure S1), In vitro stability of [$^{125}$I]c[RGDf(4-I)K] and [$^{211}$At]c[RGDf(4-At)K] (Figure S2), and Competitive binding of [$^{211}$At]c[RGDf(4-At)K] to the $\alpha_v\beta_3$ integrin (Figure S3) (PDF)

## ■ AUTHOR INFORMATION


### Corresponding Author

*E-mail: kogawa@p.kanazawa-u.ac.jp. Phone: 81-76-234-4460. Fax: 81-76-234-4459.

### ORCID

Kazuma Ogawa: 0000-0002-1691-7302

Kenji Mishiro: 0000-0002-5071-7574

Takashi Yoshimura: 0000-0002-9216-9043


### Notes

The authors declare no competing financial interest.

## ■ ACKNOWLEDGMENTS

This work was supported in part by Grants-in-Aid for Scientific Research (16H02668, 18K07630) from the Ministry of Education, Culture, Sports, Science and Technology, Japan.

## ■ REFERENCES


(1) Jadvar, H.; Chen, X.; Cai, W.; Mahmood, U. Radiotheranostics in Cancer Diagnosis and Management. *Radiology* **2018**, *286*, 388−400.

(2) Green, D. J.; Press, O. W. Whither Radioimmunotherapy: To Be or Not To Be? *Cancer Res.* **2017**, *77*, 2191−2196.

(3) Duijzentkunst, D. A. S.; Kwekkeboom, D. J.; Bodei, L. Somatostatin Receptor 2-Targeting Compounds. *J. Nucl. Med.* **2017**, *58*, 54S−60S.

(4) Eiber, M.; Fendler, W. P.; Rowe, S. P.; Calais, J.; Hofman, M. S.; Maurer, T.; Schwarzenboeck, S. M.; Kratowchil, C.; Herrmann, K.; Giesel, F. L. Prostate-Specific Membrane Antigen Ligands for Imaging and Therapy. *J. Nucl. Med.* **2017**, *58*, 67S−76S.

(5) Pandit-Taskar, N.; Modak, S. Norepinephrine Transporter as a Target for Imaging and Therapy. *J. Nucl. Med.* **2017**, *58*, 39S−53S.

(6) Hoskin, P.; Sartor, O.; O'Sullivan, J. M.; Johannessen, D. C.; Helle, S. I.; Logue, J.; Bottomley, D.; Nilsson, S.; Vogelzang, N. J.; Fang, F.; Wahba, M.; Aksnes, A.-K.; Parker, C. Efficacy and safety of radium-223 dichloride in patients with castration-resistant prostate cancer and symptomatic bone metastases, with or without previous docetaxel use: a prespecified subgroup analysis from the randomised, double-blind, phase 3 ALSYMPCA trial. *Lancet Oncol.* **2014**, *15*, 1397−1406.

(7) Kratochwil, C.; Bruchertseifer, F.; Giesel, F. L.; Weis, M.; Verburg, F. A.; Mottaghy, F.; Kopka, K.; Apostolidis, C.; Haberkorn, U.; Morgenstern, A. $^{225}$Ac-PSMA-617 for PSMA-Targeted alpha-Radiation Therapy of Metastatic Castration-Resistant Prostate Cancer. *J. Nucl. Med.* **2016**, *57*, 1941−1944.

(8) Dekempeneer, Y.; Keyaerts, M.; Krasniqi, A.; Puttemans, J.; Muyldermans, S.; Lahoutte, T.; D'huyvetter, M.; Devoogdt, N. Targeted alpha therapy using short-lived alpha-particles and the promise of nanobodies as targeting vehicle. *Expert Opin. Biol. Ther.* **2016**, *16*, 1035−1047.

(9) Zhang, Z.; Zhang, M.; Garmestani, K.; Talanov, V. S.; Plascjak, P. S.; Beck, B.; Goldman, C.; Brechbiel, M. W.; Waldmann, T. A. Effective treatment of a murine model of adult T-cell leukemia using $^{211}$At-7G7/B6 and its combination with unmodified anti-Tac (daclizumab) directed toward CD25. *Blood* **2006**, *108*, 1007−1012.

(10) Zhang, M.; Yao, Z.; Zhang, Z.; Garmestani, K.; Talanov, V. S.; Plascjak, P. S.; Yu, S.; Kim, H.-S.; Goldman, C. K.; Paik, C. H.; Brechbiel, M. W.; Carrasquillo, J. A.; Waldmann, T. A. The anti-CD25 monoclonal antibody 7G7/B6, armed with the alpha-emitter $^{211}$At, provides effective radioimmunotherapy for a murine model of leukemia. *Cancer Res.* **2006**, *66*, 8227−8232.

(11) Petrich, T.; Korkmaz, Z.; Krull, D.; Frömke, C.; Meyer, G. J.; Knapp, W. H. In vitro experimental $^{211}$At-anti-CD33 antibody therapy of leukaemia cells overcomes cellular resistance seen in vivo against gemtuzumab ozogamicin. *Eur. J. Nucl. Med. Mol. Imaging* **2010**, *37*, 851−861.

(12) Fani, M.; Nicolas, G. P.; Wild, D. Somatostatin Receptor Antagonists for Imaging and Therapy. *J. Nucl. Med.* **2017**, *58*, 61S−66S.

(13) Yoshimoto, M.; Ogawa, K.; Washiyama, K.; Shikano, N.; Mori, H.; Amano, R.; Kawai, K. alpha$_v$beta$_3$ Integrin-targeting radionuclide therapy and imaging with monomeric RGD peptide. *Int. J. Cancer* **2008**, *123*, 709−715.

(14) Brooks, P.; Clark, R.; Cheresh, D. Requirement of vascular integrin alpha v beta 3 for angiogenesis. *Science* **1994**, *264*, 569−571.

(15) Dalm, S. U.; Bakker, I. L.; de Blois, E.; Doeswijk, G. N.; Konijnenberg, M. W.; Orlandi, F.; Barbato, D.; Tedesco, M.; Maina, T.; Nock, B. A.; de Jong, M. $^{68}$Ga/$^{177}$Lu-NeoBOMB1, a novel radiolabeled GRPR antagonist for theranostic use in oncology. *J. Nucl. Med.* **2016**, *58*, 293−299.

(16) Vaidyanathan, G.; Boskovitz, A.; Shankar, S.; Zalutsky, M. R. Radioiodine and $^{211}$At-labeled guanidinomethyl halobenzoyl octreotate conjugates: potential peptide radiotherapeutics for somatostatin receptor-positive cancers. *Peptides* **2004**, *25*, 2087−2097.

(17) Vaidyanathan, G.; Affleck, D. J.; Schottelius, M.; Wester, H.; Friedman, H. S.; Zalutsky, M. R. Synthesis and evaluation of glycosylated octreotate analogues labeled with radioiodine and $^{211}$At via a tin precursor. *Bioconjugate Chem.* **2006**, *17*, 195−203.

(18) Lyczko, M.; Pruszynski, M.; Majkowska-Pilip, A.; Lyczko, K.; Was, B.; Meczynska-Wielgosz, S.; Kruszewski, M.; Szkliniarz, K.; Jastrzebski, J.; Stolarz, A.; Bilewicz, A. $^{211}$At labeled substance P (5-11) as potential radiopharmaceutical for glioma treatment. *Nucl. Med. Biol.* **2017**, *53*, 1−8.

(19) Taki, J.; Inaki, A.; Wakabayashi, H.; Imanaka-Yoshida, K.; Ogawa, K.; Hiroe, M.; Shiba, K.; Yoshida, T.; Kinuya, S. Dynamic expression of tenascin-C after myocardial ischemia and reperfusion: assessment by $^{125}$I-anti-tenascin-C antibody imaging. *J. Nucl. Med.* **2010**, *51*, 1116−1122.

(20) Ogawa, K.; Takeda, T.; Yokokawa, M.; Yu, J.; Makino, A.; Kiyono, Y.; Shiba, K.; Kinuya, S.; Odani, A. Comparison of Radioiodine- or Radiobromine-Labeled RGD Peptides between Direct and Indirect Labeling Methods. *Chem. Pharm. Bull.* **2018**, *66*, 651−659.

(21) Wilbur, D. S.; Hadley, S. W.; Grant, L. M.; Hylarides, M. D. Radioiodinated iodobenzoyl conjugates of a monoclonal antibody Fab fragment. In vivo comparisons with chloramine-T-labeled Fab. *Bioconjugate Chem.* **1991**, *2*, 111−116.

(22) Vaughan, A. T. M.; Fremlin, J. H. The preparation of astatine labelled proteins using an electrophilic reaction. *Int. J. Nucl. Med. Biol.* **1978**, *5*, 229−230.

(23) Ogawa, K.; Mizuno, Y.; Washiyama, K.; Shiba, K.; Takahashi, N.; Kozaka, T.; Watanabe, S.; Shinohara, A.; Odani, A. Preparation and evaluation of an astatine-211-labeled sigma receptor ligand for alpha radionuclide therapy. *Nucl. Med. Biol.* **2015**, *42*, 875−879.

(24) Pickett, J. E.; Váradi, A.; Palmer, T. C.; Grinnell, S. G.; Schrock, J. M.; Pasternak, G. W.; Karimov, R. R.; Majumdar, S. Mild, Pd-catalyzed stannylation of radioiodination targets. *Bioorg. Med. Chem. Lett.* **2015**, *25*, 1761−1764.

(25) Orozco, J. J.; Back, T.; Kenoyer, A.; Balkin, E. R.; Hamlin, D. K.; Wilbur, D. S.; Fisher, D. R.; Frayo, S. L.; Hylarides, M. D.; Green, D. J.; Gopal, A. K.; Press, O. W.; Pagel, J. M. Anti-CD45




DOI: 10.1021/acsomega.8b03679
ACS Omega 2019, 4, 4584−4591

radioimmunotherapy using $^{211}$At with bone marrow transplantation prolongs survival in a disseminated murine leukemia model. *Blood* **2013**, *121*, 3759−3767.

(26) Zalutsky, M. R.; Narula, A. S. A method for the radiohalogenation of proteins resulting in decreased thyroid uptake of radioiodine. *Int. J. Rad. Appl. Instrum. A* **1987**, *38*, 1051−1055.

(27) Zalutsky, M. R.; Narula, A. S. Radiohalogenation of a monoclonal antibody using an N-succinimidyl 3-(tri-n-butylstannyl)-benzoate intermediate. *Cancer Res.* **1988**, *48*, 1446−1450.

(28) Hadley, S. W.; Wilbur, D. S.; Gray, M. A.; Atcher, R. W. Astatine-211 labeling of an antimelanoma antibody and its Fab fragment using N-succinimidyl p-astatobenzoate: comparisons in vivo with the p-[$^{125}$I]iodobenzoyl conjugate. *Bioconjugate Chem.* **1991**, *2*, 171−179.

(29) Lindegren, S.; Frost, S.; Back, T.; Haglund, E.; Elgqvist, J.; Jensen, H. Direct procedure for the production of $^{211}$At-labeled antibodies with an epsilon-lysyl-3-(trimethylstannyl)benzamide immunoconjugate. *J. Nucl. Med.* **2008**, *49*, 1537−1545.

(30) Ogawa, K.; Mukai, T.; Inoue, Y.; Ono, M.; Saji, H. Development of a novel $^{99m}$Tc-chelate-conjugated bisphosphonate with high affinity for bone as a bone scintigraphic agent. *J. Nucl. Med.* **2006**, *47*, 2042−2047.

(31) Ogawa, K.; Mukai, T.; Arano, Y.; Ono, M.; Hanaoka, H.; Ishino, S.; Hashimoto, K.; Nishimura, H.; Saji, H. Development of a rhenium-186-labeled MAG3-conjugated bisphosphonate for the palliation of metastatic bone pain based on the concept of bifunctional radiopharmaceuticals. *Bioconjugate Chem.* **2005**, *16*, 751−757.

(32) Mishiro, K.; Hanaoka, H.; Yamaguchi, A.; Ogawa, K. Radiotheranostics with radiolanthanides: Design, development strategies, and medical applications. *Coord. Chem. Rev.* **2019**, *383*, 104−131.

(33) Teze, D.; Sergentu, D. C.; Kalichuk, V.; Barbet, J.; Deniaud, D.; Galland, N.; Maurice, R.; Montavon, G. Targeted radionuclide therapy with astatine-211: Oxidative dehalogenation of astatobenzoate conjugates. *Sci. Rep.* **2017**, *7*, 2579.

(34) Larsen, R. H.; Slade, S.; Zalutsky, M. R. Blocking [$^{211}$At]-astatide accumulation in normal tissues: preliminary evaluation of seven potential compounds. *Nucl. Med. Biol.* **1998**, *25*, 351−357.

(35) Garg, P. K.; Harrison, C. L.; Zalutsky, M. R. Comparative tissue distribution in mice of the alpha-emitter $^{211}$At and $^{131}$I as labels of a monoclonal antibody and F(ab')$_2$ fragment. *Cancer Res.* **1990**, *50*, 3514−3520.

(36) Chen, X.; Park, R.; Tohme, M.; Shahinian, A. H.; Bading, J. R.; Conti, P. S. MicroPET and autoradiographic imaging of breast cancer alpha v-integrin expression using $^{18}$F- and $^{64}$Cu-labeled RGD peptide. *Bioconjugate Chem.* **2004**, *15*, 41−49.

(37) Hughes, D. E.; Salter, D. M.; Dedhar, S.; Simpson, R. Integrin expression in human bone. *J Bone Miner Res* **1993**, *8*, 527−33.

(38) Singh, B.; Fu, C.; Bhattacharya, J. Vascular expression of the alpha(v)beta(3)-integrin in lung and other organs. *Am. J. Physiol.: Lung Cell. Mol. Physiol.* **2000**, *278*, L217−L226.

(39) Byk, G.; Cohen-Ohana, M.; Raichman, D. Fast and versatile microwave-assisted intramolecular Heck reaction in peptide macrocyclization using microwave energy. *Biopolymers* **2006**, *84*, 274−282.

(40) Ogawa, K.; Yu, J.; Ishizaki, A.; Yokokawa, M.; Kitamura, M.; Kitamura, Y.; Shiba, K.; Odani, A. Radiogallium complex-conjugated bifunctional peptides for detecting primary cancer and bone metastases simultaneously. *Bioconjugate Chem.* **2015**, *26*, 1561−1570.

(41) Ogawa, K.; Mukai, T.; Arano, Y.; Otaka, A.; Ueda, M.; Uehara, T.; Magata, Y.; Hashimoto, K.; Saji, H. Rhenium-186-monoamine-monoamidedithiol-conjugated bisphosphonate derivatives for bone pain palliation. *Nucl. Med. Biol.* **2006**, *33*, 513−520.



DOI: 10.1021/acsomega.8b03679
*ACS Omega* 2019, 4, 4584−4591